Fibril Formation by Primate, Rodent, and Dutch-Hemorrhagic Analogues of Alzheimer Amyloid β-Protein†

Paul E. Fraser,‡,§,∥ Jack T. Nguyen,§,∥ Hideyo Inouye,§,∥ Witold K. Surewicz,⊥ Dennis J. Selkoe,∥,# Marcia B. Podlisny,∥,# and Daniel A. Kirschner*,§,∥

Neurology Research, Children's Hospital, Boston, Massachusetts 02115, Department of Neurology, Harvard Medical School, Boston, Massachusetts 02115, Institute for Biological Sciences, National Research Council of Canada, Ottawa, K1A 0R6 Canada, and Center for Neurologic Diseases, Brigham and Women's Hospital, Boston, Massachusetts 02115

Received May 13, 1992; Revised Manuscript Received August 10, 1992

ABSTRACT: Deposition of extraneuronal fibrils that assemble from the 39–43 residue β/A4 amyloid protein is one of the earliest histopathological features of Alzheimer's disease. We have used negative-stain electron microscopy, Fourier-transform infrared (FT-IR) spectroscopy, and fiber X-ray diffraction to examine the structure and properties of synthetic peptides corresponding to residues 1–40 of the β/A4 protein of primate [Pm(1–40); human and monkey], rodent [Ro(1–40); with Arg_5→Gly, Tyr_{10}→Phe, and His_{13}→Arg], and hereditary cerebral hemorrhage with amyloidosis of the Dutch type (HCHWA-D) [Du(1–40); with Glu_{22}→Gln]. As controls, we examined a reverse primate sequence [Pm*(40–1)] and an extensively substituted primate peptide [C(1–40); with Glu_3→Arg, Arg_5→Glu, Asp_7→Val, His_{13}→Lys, Lys_{16}→His, Val_{18}→Asp, Phe_{19}→Ser, Phe_{20}→Tyr, Ser_{26}→Pro, Ala_{30}→Val, Ile_{31}→Ala, Met_{35}→norLeu, Gly_{38}→Ile, Val_{39}→Ala, and Val_{40}→Gly]. The assembly of these peptides was studied to understand the relationship between species-dependent amyloid formation and β/A4 sequence and the effect of a naturally occurring point mutation on fibrillogenesis. The three N-terminal amino acid differences between Pm(1–40) and Ro(1–40) had virtually no effect on the morphology or organization of the fibrils formed by these peptides, indicating that the lack of amyloid deposits in rodent brain is not due directly to specific changes in its β/A4 sequence. β-Sheet and fibril formation, judged by FT-IR, was maximal within the pH range 5–8 for Pm(1–40), pH 5–10.5 for Du(1–40), and pH 2.5–8 for Ro(1–40). At pH 2.5, β-sheet formation also occurred though at greatly reduced rates for both Pm(1–40) and Du(1–40), indicating the importance of both hydrophobic and electrostatic interactions in amyloid formation. At high pH, the β-conformation persisted much more in Du(1–40) than in Ro(1–40) and not at all in Pm(1–40). The single substitution of Glu_{22}→Gln in Du(1–40) enhanced fibril stability under electron microscopy conditions as demonstrated by visualization of fibrils in the absence of any stabilizing pretreatment such as glutaraldehyde fixation. A decrease in electrostatic potential and a possible enhancement of interactions between uncharged side chains adjacent to the core region of β/A4 (residues 17–21) could account for the greater stability of Du(1–40) fibrils. C(1–40) peptide, which contains numerous substitutions, assembled into fibrils that differed only slightly in morphology from naturally occurring β/A4 proteins; and Pm*(40–1) only formed amorphous aggregates, with no fibrillar structure identifiable. X-ray diffraction of the various assemblies formed by Pm(1–40), Ro(1–40), Du(1–40), and C(1–40) indicated the cross-β conformation typical for amyloid. Correlation of our findings with the neurotoxicity data suggests tha β/A4 neurotoxicity may be related not only to the correct sequence but also to the proper folding into a cross-β fibril.

The histopathology of Alzheimer's disease (AD) is distinguished by extensive neuronal death accompanied by filamentous protein deposits. Abnormal fibers accumulate as cerebrovascular amyloid (CVA) within cortical and meningeal microvessels (capillaries, arterioles, and some venules), dense neuropil senile plaques (SP), and intraneuronal neurofibrillary tangles [reviewed by Selkoe (1991)]. The major protein constituent of CVA and SP is 39–43 residue protein, the amyloid β-protein (denoted β/A4) (Glenner & Wong, 1984a,b; Masters et al., 1985a,b; Selkoe et al., 1986). Subsequent cloning (Kang et al., 1987) and biochemical studies (Selkoe et al., 1988; Dyrks et al., 1988) have demonstrated that β/A4 is derived from a ~120–140-kDa glycosylated integral membrane precursor protein, βAPP, which can exist in at least three different forms (695, 751, and 770 residues) as a result of alternative splicing of a Kunitz-type protease inhibitor domain (Ponte et al., 1988; Tanzi et al., 1988; Kitaguchi et al., 1988). The importance of β/A4 in AD also derives from the occurrence of point mutations in some familial cases (Goate et al., 1991; Murrell et al., 1991), the finding that individuals with trisomy 21 (Down's syndrome) develop AD pathology (Mann & Esiri, 1989), and its apparent neuronal toxicity (Yankner et al., 1990; Koh & Cotman, 1991; Mattson et al.,

† This research was supported by the American Health Assistance Foundation (D.A.K.), National Institutes of Health Grant AG-08572 (to D.A.K.) from the National Institute of Aging, and a grant from the Foundation for Neurologic Disease (to D.J.S). P.E.F. is a postdoctoral fellow of the Medical Research Council of Canada. Some of the work was carried out in facilities related to the Mental Retardation Research Center of Children's Hospital, and was supported by Core Grant HD-18655 from the National Institutes of Health.

* Corresponding Author: Neurology Research—Enders 2, Children's Hospital, 320 Longwood Ave., Boston, MA 02115. Telephone, (617) 735-6103; FAX, (617) 730–0636; E-mail, dkirsch@amy.tch.harvard.edu.

‡ Current address: Centre for Research in Neurodegenerative Diseases, Tanz Neuroscience Building, University of Toronto, Toronto, M5S 1A8 Canada.

§ Children's Hospital.

∥ Harvard Medical School.

⊥ National Research Council of Canada.

Brigham and Women's Hospital.

0006-2960/92/0431-10716$03.00/0

1992) and potential link with neuritic pathology (Kowall et al., 1991).

How β/A4 is generated and why its deposition as amyloid is largely restricted to aged primates may involve a combination of altered βAPP processing and the unusual amyloidogenic properties of the human β/A4 sequence. This notion is supported by the observation that constitutive βAPP cleavage (Sisodia et al., 1990; Esch et al., 1990; Estus et al., 1992) occurs at Lys_{612}–Leu_{613} (βAPP_{695} numbering; or Lys_{16}–Leu_{17}, β/A4 numbering) to produce a soluble, secreted protein (Weidemann et al., 1989; Palmert et al., 1989; Oltersdorf et al., 1990) previously identified as protease nexin II (Oltersdorf et al., 1989; Van Nostrand et al., 1989). During brain aging and particularly in AD, an alternative upstream cleavage at Met_{596}–Asp_{597} (Met_0–Asp_1, β/A4 numbering) contributes to the release of the downstream β/A4 fragment that accumulates as insoluble amyloid deposits. Alternative proteolysis could occur normally and be influenced by posttranslational modifications such as phosphorylation (Buxbaum et al., 1990), changes in local protease inhibitors such as α_1-antichymotrypsin (ACT) (Abraham et al., 1988; 1990), mutations within β/A4 that affect the product or stability of βAPP fragments as, for example, in hereditary cerebral hemorrahge with amyloidosis of the Dutch type (HCHWA-D) (Levy et al., 1990), or possible lysosomal defects (Benowitz et al., 1989; Cataldo et al., 1991; Golde et al., 1992).

Immunocytochemistry shows that the earliest form of β/A4 deposits has a diffuse, nonfibrillar (amorphous) morphology (Joachim et al., 1989; Yamaguchi et al., 1989; Rozemuller et al., 1989) and cannot be visualized by Congo red or thioflavin S. Because the classical senile (neuritic) plaques do exhibit these tinctorial properties and contain clearly distinguishable fibrils that have widths of 60–100 Å and a cross-β conformation (Kirschner et al., 1986), morphological and conformational transitions are likely involved in the presumed maturation of diffuse plaques to senile plaques. Several investigations have approached the question of amyloid assembly and structure by using synthetic peptide fragments to determine the properties of defined β/A4 regions. Early studies (Castaño et al., 1986; Kirschner et al., 1987; Gorevic et al., 1987) on the extramembranous portion of β/A4 determined that the N-terminal 28 residues were sufficient to produce fibrils resembling amyloid in vivo. More recent studies using progressively longer β/A4 analogues (Fraser et al., 1991a), peptides derived from the hydrophobic C-terminal (Halverson et al., 1990), and full-length β/A4 species (Fraser et al., 1991b; Hilbich et al., 1991a,b; Barrow & Zagorski, 1991; Burdick et al., 1992) have suggested the importance of hydrophobic and electrostatic interactions in the polymerization and stabilization of β/A4 fibrils.

To understand (i) the relationship between the β/A4 sequence in primates and rodents and species-variable amyloidosis, (ii) the effect of a naturally occurring point mutation on fibrillogenesis, and (iii) the link between peptide sequence and possible neuronal toxicity, we have undertaken a comparative study of five synthetic peptides corresponding to the primate, rodent, and HCHWA-D β/A4 sequences and to an extensively substituted sequence and reverse sequence for the primate form. Using negative-stain electron microscopy, Fourier-transform infrared (FT-IR) spectroscopy, and fiber X-ray diffraction, we have investigated the morphology, structure, and stability of the assemblies formed by these peptides. We found that sequence differences between primate and rodent did not alter β/A4 fibril morphology but did result in a slightly more amyloidogenic peptide for the rat sequence

```
1   5   10  15  20  25  30  35  40
DAEFRHDSGYEVHHQKLVFFAEDVGSNKGAIIGLMVGGVV      Pm(1-40)
----G----F--R--------------------------      Ro(1-40)
--------------------Q----------------------  Du(1-40)
--R-E-V-----K--H-DSY-----P---VA---L--IAG      C(1-40)
VVGGVMLGIIAGKNSGVDEAFFVLKQHHVEYGSDHRFEAD      Pm*(40-1)
```

FIGURE 1: Sequences of the synthetic Alzheimer amyloid β-peptides corresponding to residues 1–40 of primate [Pm(1–40)], rodent [Ro-(1–40)], hereditary cerebral hemorrhage with amyloidosis of the Dutch type [HCHWA-D; Du(1–40)] hemorrhagic mutation, and substituted combination [C(1–40)] proteins. L denotes a norleucine residue. [See Podlisny et al., (1992) for details on peptide synthesis and purity assay].

and that the single change in residue between primate and HCHWA-D (Glu_{22}→Gln) had an even more profound effect on fibril stability. The control peptide with the reverse human sequence appeared amorphous and did not form fibrils under any conditions. The substituted peptide, which is reported to have lower in vivo toxicity than a primate 1–40 peptide (Kowall et al., 1991), did not exhibit reduced fibril formation.

MATERIAL AND METHODS

Peptide Synthesis and Purification. Amyloid β-peptides corresponding to residues 1–40 of primate [Pm(1–40)], rodent [Ro(1–40)], HCHWA-D [Du(1–40)], substituted [C(1–40)], and reverse [Pm*(40–1)] sequences were synthesized by solid-phase methods in the Department of Biological Chemistry and Molecular Pharmacology, Harvard Medical School (Figure 1). Human and monkey β/A4 peptides [Pm(1–40)] were synthesized using the sequences reported by Kang et al. (1987) and Podlisny et al. (1991). Ro(1–40) contained three substitutions, Arg_5→Gly, Tyr_{10}→Phe, and His_{13}→Arg, as reported for mouse (Yamada et al., 1987, 1989) and for rat (Shiver et al., 1988). Du(1–40) contained a single Glu_{22}→Gln change, as determined by Levy et al. (1990). The substituted peptide, C(1–40), contained 15 randomly selected substitutions. All peptides were purified by C-18 reverse-phase HPLC to >95% as confirmed by amino acid analysis and had the predicted molecular weight by mass spectrometry.

Electron Microscopy. Negative-stained fibrils were obtained by two different methods. In one technique, pioloform and carbon-coated grids were floated on peptide solutions (1 mg/mL in buffer or distilled water), air-dried, and fixed by exposure to glutaraldehyde vapor (2%; 15–20 min) to stabilize the assemblies (Caputo et al., 1992). In the second procedure, which followed the microdialysis technique described by Hilbich et al., (1991), peptides were dialyzed against several changes of phosphate-buffered saline (PBS) over a period of 2–3 days and then fixed. Specific buffers and peptide preparations are given in the figure legends. Assemblies after fixation or dialysis were stained with either aqueous uranyl acetate (2% w/v) or phosphotungstic acid (1% w/v) and visualized in a JEOL 100S or 1200EX electron microscope operated at 80 kV. Fibril dimensions were calibrated using tropomyosin paracrystals kindly provided by Dr. C. Cohen (Brandeis University, Waltham, MA).

Fourier-Transform Infrared Spectroscopy. IR spectra were collected on a Digilab FTS-60 instrument operated at 2 cm^{-1} resolution. Peptide solutions of typically 3–5 mg/mL were prepared in D_2O with subsequent pD adjustments being made with DCl or NaOD. Electrode readings were uncorrected for deuterium effects. Sample aliquots (~5 μL) were placed in demountable cells containing CaF_2 windows separated by 50-μm teflon spacers. Spectra were generally recorded following a 20-min incubation at each pD value at room temperature. For kinetic studies, spectra were recorded periodically from

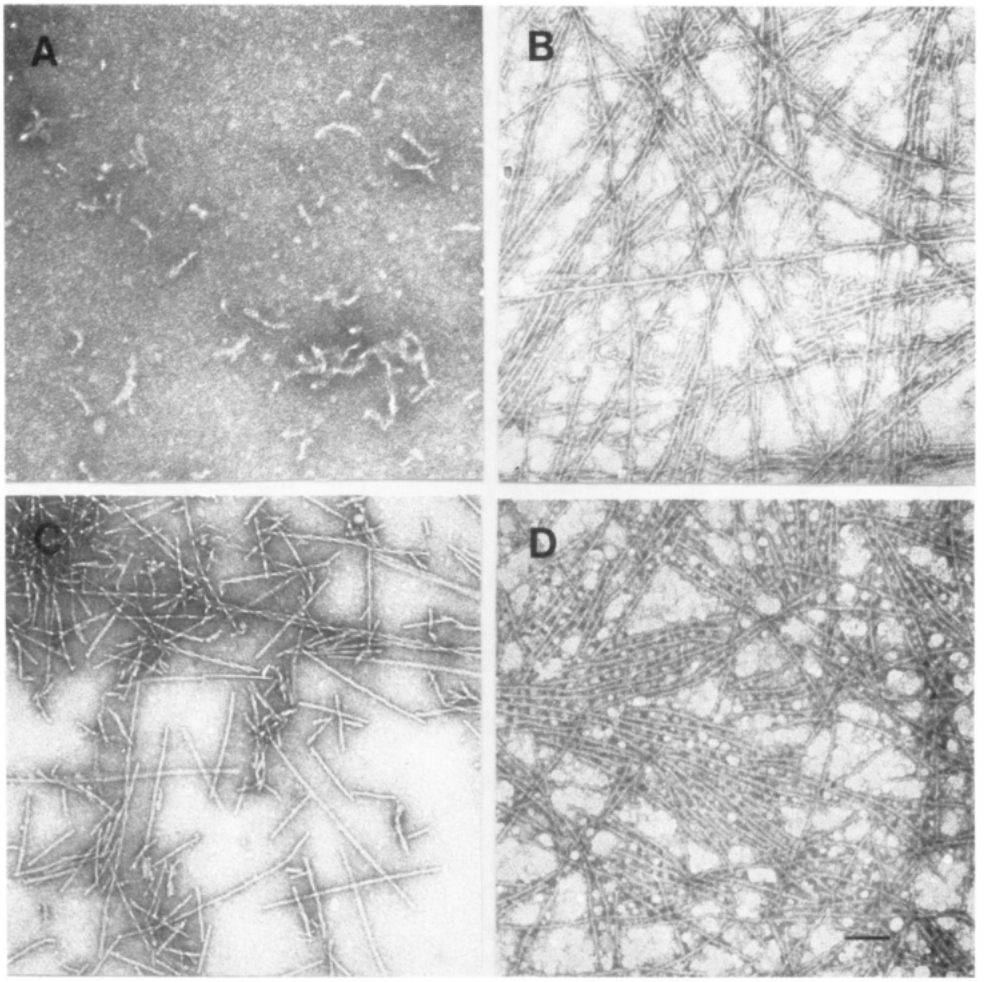

FIGURE 2: Electron micrographs of negative-stained preparations of fibrils assembled from β/A4 analogues. (A) Peptide Pm(1–40) applied to a grid and stained directly with no prior treatment. (B) Peptide Pm(1–40) fibrils that have been stabilized by microdialysis and pre-fixing with 2% glutaraldehyde vapor; morphologically identical fibers were observed with Ro(1–40) peptide with direct fixing but without the necessity of prior dialysis. (C) Du(1–40) prepared in aqueous solution; no dialysis and without vapor fixation. (D) Peptide C(1–40). All samples were prepared from a 1–2 mg/mL solution in 10 mM Tris buffer, pH 7, and stained with phosphotungstic acid (1% w/v). The scale bar is 1000 Å.

10 min to 30 h with samples incubating in the IR cell at room temperature. To eliminate overlapping trifluoroacetate (TFA) bands at ~1675 cm^{-1}, all HPLC purified peptides were repurified using 10 mM HCl in the mobile phase.

Fiber X-ray Diffraction. Peptide diffraction samples were prepared from unbuffered aqueous solutions (~10 mg/mL) that were slowly dried, under ambient conditions, in siliconized 0.7-mm diameter thin-walled glass X-ray capillaries (Charles Supper Co., Natick, MA). Fibril orientation was induced using a 2-T permanent magnet. Diffraction patterns were recorded on Kodak DEF film using double mirror focused Cu Kα radiation generated by an Elliot GX-20 rotating anode (Marconi Avionics, U.K.) with specimen to film distances of 71 and 174 mm. Exposure times were from 1–3 days, and the observed reflections were measured as previously described (Fraser et al., 1991a,b).

RESULTS

"Dutch" Peptide Formed the Most Stable Fibrils. Solutions of Pm(1–40) or Ro(1–40) at 1 mg/mL (in water or 10 mM buffer) applied directly to grids with no pretreatment and negatively stained revealed small, indistinct fibrils ranging in length from 1000 to 2000 Å (Figure 2A). To obtain well-defined, nonbranching, 80-Å diameter fibrils required both microdialysis and fixation with glutaraldehyde vapor for Pm(1–40), while only fixation sufficed for Ro(1–40) (Figure 2B). The Pm(1–40) and Ro(1–40) fibrils, which were indistinguishable from one another, were about 5000 Å or more in length. Direct solubilization of Pm(1–40) with PBS yielded precipitates that contained only amorphous structures (not shown). Samples prepared by microdialysis and negative-stained without fixation contained fibrils that were considerably shorter than those vapor-fixed. The negatively stained fibrils formed by Pm(1–40) in this study were consistently more distinct than those observed in our previous study (Fraser et al., 1991a), in which the peptide was from a different source and vapor fixation on the grid prior to staining was not used.

There was no apparent difference in the time course of fibril formation for Du(1–40) versus Pm(1–40) or Ro(1–40), on the basis of the relative number and morphology of the fibrils, as all could be observed within 30 min after their solubilization at 1 mg/mL in aqueous solutions. Of the three naturally occurring peptides, however, only the Du(1–40) assemblies were sufficiently stable that fibrils could be obtained directly without the need for vapor fixing or microdialysis. The resulting fibrils were nonbranching and of variable length (Figure 2C). Often they were highly twisted having a ~360-Å pitch and minimum and maximum widths of about 60 and 120 Å (Figure 2C).

Formation of stable fibrils by C(1–40) did not require microdialysis or fixation, and the fibrils showed only infrequent twisting (Figure 2D). In contrast with the four other peptides,

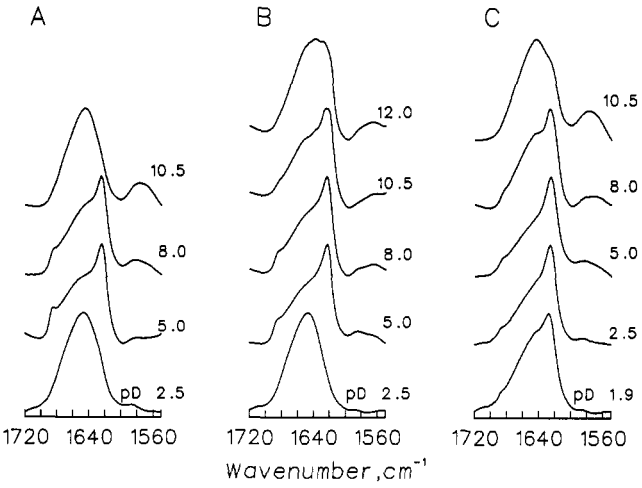

FIGURE 3: Fourier-transform infrared spectra of β/A4 peptides as a function of pD. (A) Pm(1–40) preparations showing the transition from random conformation (~1645 cm^{-1}) at pD 2.5 to β-conformation at intermediate pD 5–8 to random conformation again at pD 10.5. (B) Du(1–40) shows a similar transition from random to β-conformation, except that the β-structure persists at high pD. (C) Formation of β-sheet by Ro(1–40) indicating the presence of secondary structure at low pD. A small β-sheet component also remains at pD 10.5 as seen by the slight intensity at ~1620 cm^{-1}. All samples are in D_2O; pH electode uncorrected for deuterium effects.

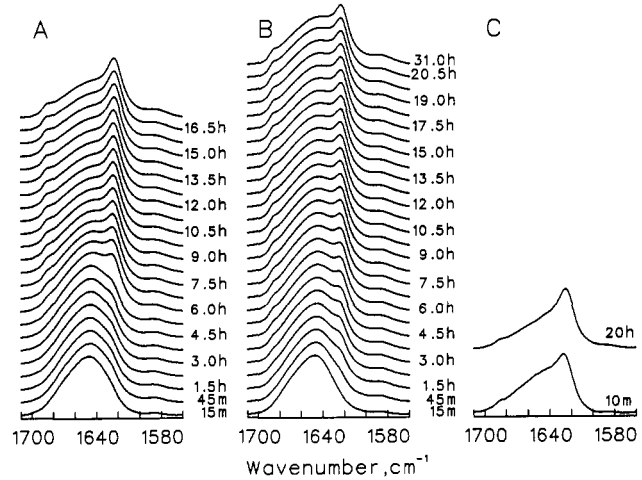

FIGURE 4: Fourier-transform infrared spectra of β/A4 peptides as a function of incubation time at pD 2.5. (A) Kinetics of Pm(1–40) assembly from random to β conformation over a period of 18 h. (B) Similar kinetics observed for Glu_{22}→Gln substituted Du(1–40) analogue. (C) Ro(1–40) assembly appears time-independent as only slight changes in β-conformation were observed during incubation from 10 min to 20 h.

no identifiable fibrils but only amorphous aggregates were present in negatively stained preparations of the reverse primate peptide Pm*(40–1), even after fixation on the grid or microdialysis. The relative stability of the peptide fibrils was Du/C > Ro > Pm based on whether pretreatment was necessary to visualize fibrils in the electron microscope.

Fibril Formation and Kinetics of β-Conformation Depended on pH. Several reports have indicated variations in β/A4 peptide β-sheet conformation, aggregation, and solubility as a function of pH (Barrow & Zagorski, 1991; Fraser et al., 1991a,b; Burdick et al., 1992). Using FTIR, we assessed the pH and time dependence of Pm(1–40), Du(1–40), and Ro(1–40) to fold into the β-conformation (Figures 3 and 4).

Pm(1–40) at pD 2.5 existed as a random conformation as shown by a single broad peak centered at ~1645 cm^{-1} (Figure 3A). Titration of the same sample to pD 5.0 resulted in the conversion of Pm(1–40) into a β-sheet conformation as indicated by both the low (~1625 cm^{-1}) and high (~1685 cm^{-1}) frequency bands. Further titration to pD 8.0 resulted in a slight increase in random conformation but with the majority of peptides maintaining a β-sheet conformation. Only under very basic conditions (pD 10.5) was the β-conformation completely eliminated. At the low pD range, there were not significant differences between Pm(1–40) and Du(1–40) samples; however, at high pD (10.5–12), an appreciable amount of β-conformation persisted in Du(1–40) (Figure 3B).

At pD 1.9, Ro(1–40) existed as a mixture of random and β-sheet conformers (Figure 3C). Subsequent increases to pD 2.5–5.0 caused a further shift toward the β-sheet conformation with a parallel decrease in the random conformation. At pD 8.0 this trend was reversed to some degree with a decrease in the amount of β-conformation; however, Ro(1–40) could not be as completely randomized as Pm(1–40) as indicated by the persistence of a slight shoulder in the β region at pD 10.5.

Although Pm(1–40) and Du(1–40) did not immediately fold into a β-conformation at pD 2.5, increasing the incubation time did reveal a time-dependent aggregation (Figure 4A). After ~3 h, Pm(1–40) began a slow conversion from a random to β-conformation, which continued over 16–18 h with the β eventually dominating. Du(1–40) at pD 2.5 displayed nearly identical assembly kinetics as Pm(1–40) (Figure 4B). By contrast with this gradual conversion, Ro(1–40) at pD 2.5 assumed a β-conformation already within the first 10 min of incubation (Figure 4C) and remained virtually unchanged for at least 20 h.

The pH dependence of fibril assembly for Pm(1–40) and Ro(1–40) was also determined by electron microscopy. Fibrils were prepared either directly in solutions buffered at pH 2.5 (glycine buffer) and pH 9 [buffered with 3(cyclohexylamino)-1-propanesulfonic acid, or CAPS] and stabilized by fixing or by dialysis against similarly buffered solutions. For Pm(1–40) at pH 2.5 and with no incubation, a small number of short (~500 Å), nonuniform, highly curved fibrils were observed (Figure 5A) that became substantially longer and straighter after 24 h (Figure 5B). Ro(1–40) formed fibrils at both pH 2 and 9 and at pH 9 (Figure 5C) exhibited more fibril twisting, and the fibrils were even shorter than those at the lower pH. Similar time- and pH-dependent aggregation of β/A4 peptides as determined by gel electrophoresis has recently been described (Burdick et al., 1992).

Peptides Folded into Cross-β Conformation. Isolated amyloid fibrils (Eanes & Glenner, 1968; Glenner et al., 1974; Kirschner et al., 1986) and many in vitro peptide assemblies (Castaño et al., 1986; Gorevic et al., 1987; Kirschner et al., 1986; Halverson et al., 1990; Fraser et al., 1991a,b; Hilbich et al., 1991a,b; Barrow & Zagorski, 1991) exhibit a characteristic cross-β conformation composed of β-pleated sheets arranged with the hydrogen-bonding direction parallel to the fibril axis. The β-sheets can associate via interresidue interactions to produce the organized fibrils seen by negative-stain electron microscopy. If the fibrils can be oriented, either by sedimentation or application of a magnetic field, then a distinctive diffraction pattern is observed that contains a ~4.7-Å meridional reflection (corresponding to the hydrogen-bonding distance between chains) and a ~10-Å equatorial reflection (corresponding to the intersheet spacing). In addition, small-angle reflections may be present on either axis, resulting from periodic fluctuations along the fibril axis and/or regular lateral packing of fibrils.

Unoriented lyophilized samples of the peptides Pm(1–40), Du(1–40), Ro(1–40), and C(1–40) all displayed two rings having spacings 4.7 and 10.5 Å, indicative of the hydrogen-

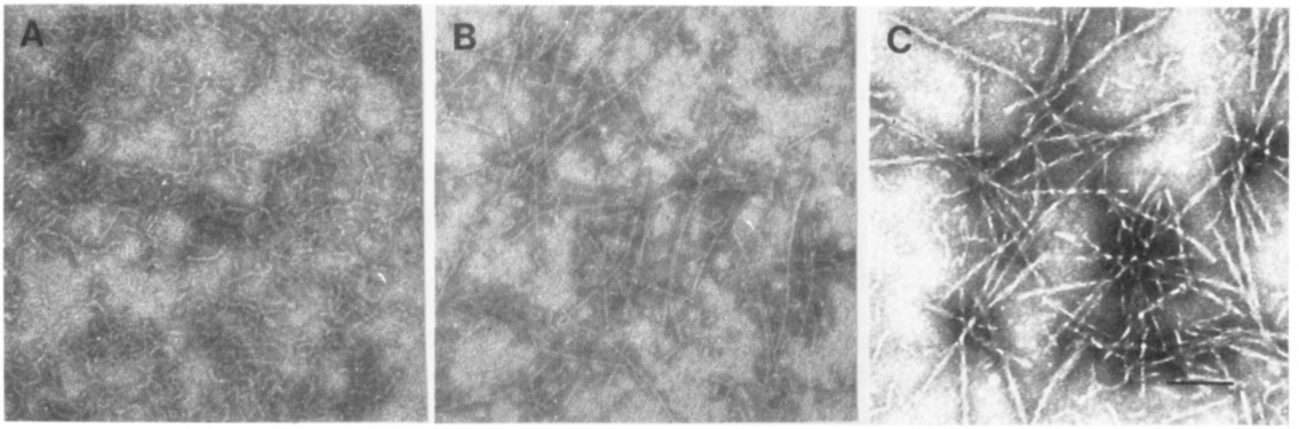

FIGURE 5: Electron micrographs of negative-stained preparations of fibrils assembled from β/A4 analogues in buffered solutions at different pH. (A) Pm(1–40) in 10 mM glycine, pH 2.5, with no incubation. (B) Pm(1–40) sample at pH 2.5 following a 24-h incubation shows long, well-defined fibrils. (C) Ro(1–40) peptide sample in 10 mM CAPS, pH 9.0; similar highly twisted fibrils were observed at pH 2.5. Lyophilized peptides were suspended in the appropriate buffer at concentrations of 1–2 mg/mL and negative-stained with phosphotungstic acid (1% w/v). The scale bar is 1000 Å.

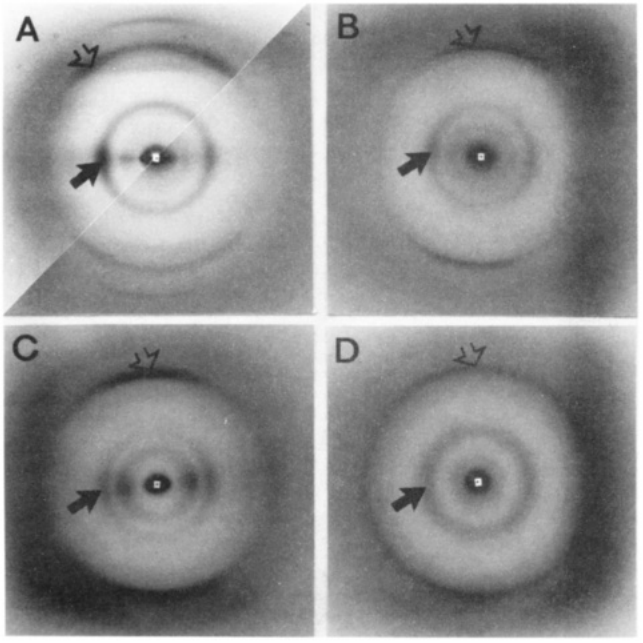

FIGURE 6: X-ray diffraction patterns of β/A4 analogues. Oriented X-ray diffraction patterns from partially dried preparations of fibrils assembled from (A) Ro(1–40) [Pm(1–40) exhibited virtually identical reflections and intensities]; (B) Du(1–40); (C) C(1–40); (D) Pm*-(40–1). The orthogonal orientations of the reflections corresponding to hydrogen-bonding (meridional 4.7 Å; open arrow) and intersheet (equatorial 10 Å; closed arrow) dimensions are consistent with the cross-β conformation. Spacings of observed reflections are given in Table I.

Table I: Major X-ray Diffraction Spacings (Å) and Intensities for Oriented Fibrils Formed by Different 40-mer β/A4 Peptides[a,b]

Pm(1–40)[c]	Ro(1–40)	Du(1–40)	C(1–40)	Pm*(40–1)
57 (M, w)		108 (E, vs)	95 (M, s)	
48 (E, vs)	46 (E, vs)	42 (E, s)	55 (E, vs)	51 (E, vs)
	21 (E, w)			22 (c, vw)
15 (E, w)	16 (E, w)	17 (E, w)	14 (E, s)	
11 (M, w)	12 (M, w)			
9.3 (E, s)	9.2 (E, s)	10 (E, s)	9.6 (E, s)	10 (E, w)
5.8 (M, w)	5.8 (M, w)		5.7 (E, vw)	
4.6 (M′, s)	4.7 (M′, s)	4.8 (M, s)	4.7 (M, s)	4.7 (M, s)
			4.5 (M, w)	
3.9 (M, s)	3.9 (M, s)	3.8 (M′, w)	3.7 (M′, vw)	3.8 (c, w)

[a] Pm(1–40), primate; Ro(1–40), rodent; Du(1–40), Dutch-hemorrhagic; C(1–40), substituted; Pm*(40–1), reverse primate sequence. [b] The reflections are identified as either meridional (M) or equatorial (E), which correspond, respectively, to the fiber direction and to the direction normal to the fiber axis (or rotation axis). Off-meridional reflections are denoted by M′; c denotes a circular reflection. Intensities were arbitrarily designated as very strong (vs), strong (s), weak (w), or very weak (vw) as judged by eye. [c] For Pm(1–40) the small-angle reflections on the equator roughly correspond with the 1st, 2nd, 3rd, and 5th orders of ~45 Å, while on the meridian the three sharp reflections indexed as 1st, 2nd, and 3rd orders of 11.4 Å.

bonding and intersheet features of β-sheet conformations [not shown; see Fraser et al. (1991a)]. By contrast, the reverse peptide Pm*(40–1) showed only the ~10-Å spacing. After solubilization of peptide followed by gradual dehydration and orientation, the peptide assemblies [except for Pm*(40–1); see below] all displayed a cross-β conformation as indicated by the clearly distinguishable orthogonal reflections at spacings of 9–10 and ~4.7 Å (Figure 6A,B). Pm(1–40) and Ro(1–40) gave similar diffraction patterns suggesting that their assemblies were indistinguishable in both conformation and morphology (Figure 6A). The major features (Table I) were intense, small-angle (~45–50 Å), and intersheet (~9 Å) reflections on the equator, plus hydrogen-bonding (~4.7 Å) spacings off the meridian. These features indicate that the β-pleated sheet is the major structural motif of the fibrils. The off-meridional hydrogen-bonding reflection was atypical, however, and the amount of angular deviation from the meridian suggests that the β-strands were tilted by ~36° from their usual perpendicular orientation relative to the long axis of the fibril. The fiber direction was parallel to the 3.8-Å reflection on the meridian, which is indexed as (210) assuming an orthogonal unit cell (Kirschner et al., 1987). Lateral packing of the fibrils arising from long-range macromolecular interactions could give rise to the small-angle reflection on the equator. There was also a weak reflection at ~57 Å on the meridian, which has previously been recorded from another β-(1–40) sample (Fraser et al., 1991a) and could correspond to an axially repeating unit consisting of ~12 hydrogen-bonded β-strands.

Du(1–40) samples did not orient during gradual dehydration to the same degree as did Pm(1–40) or Ro(1–40), but the basic features and spacings were similar (Figure 6B). The orthogonal orientation of the hydrogen-bonding and intersheet reflections was indicative of a cross-β conformation, although, unlike Pm(1–40) or Ro(1–40), the centering of the former on the meridian suggests that the β-strands of the Du(1–40) fibrils were not significantly tilted from their orientation perpendicular to the fiber axis. In addition to the small-angle equatorial reflection at ~42 Å, which was similar to that of Pm(1–40) and Ro(1–40), there was an intensity maximum

on the equator at ~108 Å, suggesting a difference in lateral packing or organization of the substructure of the fibrils. Further X-ray diffraction studies on differentially hydrated samples would be required to resolve whether this latter spacing, which was partially obscured by the strong central scatter, is related to inter- or intrafibril packing. No small-angle meridional scatter was detected. Overall, however, the X-ray pattern was very similar to that for β-(1–38), which we have previously published (Fraser et al., 1991a).

C(1–40), with its large number (15) of amino acid substitutions, including both conservative and nonconservative changes, gave a cross-β X-ray pattern (Figure 6C) similar to that for Du(1–40). There was also a spacing at ~95 Å on the meridian, suggesting an axially repeating unit about twice the extent of that for Pm(1–40) and Ro(1–40). Pm*(40–1), the peptide with the sequence reversed to that of Pm(1–40), gave an X-ray pattern that was almost completely disoriented (Figure 6D). Spacing consistent with the cross-β conformation were observed at 4.7 Å (hydrogen-bond spacing) on the meridian and 10.1 Å on the equator. While strong small-angle equatorial scatter was present at ~51 Å, no small-angle meridional scatter was detected. Thus, while the macromolecular structure of the peptide assembly was amorphous, there was evidence for β-pleated sheet structure at the molecular level.

DISCUSSION

Amyloid Fibril Formation and β/A4 Species Variations. Rodent β/A4 as compared to the primate sequence contains one nonconservative (Arg_5→Gly) and two relatively conservative (Tyr_{10}→Phe and His_{13}→Arg) substitutions (Yamada et al., 1987, 1989; Shivers et al., 1988; Podlisny et al., 1991). A recent electron microscopic and spectroscopic study of human and rodent β/A4 indicates that these sequences share similar structural and fibril-forming properties (Hilbich et al., 1991b). Our X-ray diffraction observations that Pm(1–40) and Ro(1–40) are virtually indistinguishable in structure further substantiate the conclusion that the lack of amyloid deposits in rodents is not due directly to specific changes in the β/A4 peptide sequence. Differences between these two peptides were found, however, by FT-IR, which indicated a slightly more stable β-conformation at low and high pH for the rodent analogue. This finding is consistent with the His_{13}→Arg substitution, which is in the region of the β/A4 protein that is thought to be important in electrostatic interactions (Fraser et al., 1991a). Such interactions would be enhanced by the higher pK_a (~12) of Arg as compared to His (pK_a ~ 6). In kinetics measurements, FT-IR revealed that the rodent peptide formed the β-conformation much more readily than did the primate, i.e., in minutes rather than hours. Therefore, the rodent β/A4 peptide appears to be more amyloidogenic in vitro than the corresponding primate sequence.

Although the ability of rodent β/A4 to assemble in vitro into amyloid fibrils is unaffected, it is possible that sequence changes in rodent βAPP (both within and outside of the β/A4 region) could underlie the failure of rodents generally to develop spontaneously AD-like amyloid plaques, especially considering that mice transfected with human βAPP apparently produce some deposits resembling diffuse β/A4 plaques (Quon et al., 1991). The particular sequence changes in rodent βAPP may affect βAPP processing or alter the binding of secondary tissue components (Podlisny et al., 1991). For example, it has been proposed that the N-terminal region of β/A4 is an α_1-antichymotrypsin (ACT) binding site due to its homology with the active sites of serine proteases (Asp_7–Ser_8–Gly_9) (Dressler et al., 1989). ACT colocalizes with amyloid plaque cores and nonfilamentous diffuse plaques in AD but not with any other type of amyloid and may therefore play a role in the initiation of amyloid fibril formation and deposition (Abraham et al., 1988, 1990). Although the rodent substitutions are not directed to the Asp_7–Ser_8–Gly_9 region, neighboring changes, particularly the nonconservative Arg_5→Gly, may adversely affect ACT binding or alter processing through an amyloidogenic pathway. These possible species differences have yet to be documented.

Kinetics of Amyloid Fibril Formation and pH Dependence. Understanding the mechanism of β/A4 folding and identifying the essential residues in this process is crucial not only to explain amyloid formation but also to developing a rationale for preventing or inhibiting its formation. It has recently been proposed (Fraser et al., 1991a; Barrow & Zagorski, 1991; Burdick et al., 1992) that the ionization state of key residues, as shown by the pH dependence of β/A4 peptides β(1–28), β(1–39), and β(1–43), affects the assembly of the β-strands. The finding that oligomeric β-conformation and peptide fibrils were observed only at intermediate pH indicates the influence of His–Asp/Glu salt bridges on the stabilization of the β-sheets and, ultimately, fibril assembly. Similar properties have also been reported for native, isolated senile plaque amyloid (Masters et al., 1985).

Our current observations at different values of pH confirm that electrostatic interactions at neutral pH produce the optimal conditions for fibril formation. However, as demonstrated with the 1–40 analogues, the lack of these interactions at low or high pH does not completely inhibit fibril assembly, underscoring the importance of hydrophobic interactions. Ionic interactions have been questioned by Hilbich et al. (1991), who found that β/A4 peptides containing hydrophobic substitutions for His_{13}–His_{14} (Ala–Ala or Ala–Ile) exhibit enhanced propensities to form insoluble fibrils. However, such substitutions would increase the hydrophobicity within this crucial core region of the β-strand, leading to enhanced fibril assembly, as shown by the peptide having the HCHWA-D substitution. Exchanging residues with different ionic characteristics, for example, His→Asp or Asp→Lys, should test the role of electrostatic interactions in stabilizing intermolecular β-sheet polymerization. Peptides containing such changes are currently under investigation.

Amyloid Peptides and Toxicity. Synthetic β/A4 peptides have variously been reported to (1) exert direct neuronal toxicity both in vitro (Yankner et al., 1990; Pike et al., 1991) and in vivo (Kowall et al., 1991; McKee et al., 1991), (2) potentiate excitotoxic damage in vitro (Koh et al., 1990; Mattson et al., 1992), and (3) show little effect in vivo (Podlisny et al., 1992; Stephenson et al., 1991). Technical differences in methodology, animal strains, species, and age as well as differences among peptides synthesized and purified in various laboratories may explain the current lack of agreement about the biological activity of β/A4. Indeed, the Pm(1–40), C(1–40), and reverse Pm*(40–1) peptides when injected into young adult monkey cortex did not produce acute neurotoxicity 2 weeks postinjection (Podlisny et al., 1992). A different batch of synthetic β/A4 1–40 peptide that produced shorter fibrils in a previous study (Faser et al., 1991a) has been reported to be directly toxic in several different systems: in vitro, differentiated rat neurons (Yankner et al., 1990) and in vivo, adult rat cortical and hippocampal neurons after 3–7 days (Kowall et al., 1991) and aged monkeys after 2 weeks (McKee et al., 1991). In one of these studies, the C(1–40) peptide

examined in the current study resulted in ~60% of the cytotoxicity produced by a β/A4 1–40 peptide in rat cortex (Kowall et al., 1991).

Negative-stain electron microscopy and X-ray diffraction in the present study have shown that C(1–40) exhibited some minor differences in structure such as subtle changes in fibril morphology and orientation of the β-strands. Overall, however, its cross-β conformation and ability to assemble into fibrous polymers was not inhibited by the numerous amino acid substitutions. By contrast, Pm*(40–1) was more easily distinguished from the other peptides, particularly in its lack of a clear fibrillar ultrastructure by electron microscopy and less-detailed, though still β-type, X-ray pattern. Thus, the reverse peptide assembled into β-pleated sheets, but these did not assemble further into organized amyloid-like fibrils. Pm*-(40–1) may, therefore, be a more suitable control than C(1–40) in toxicity studies. A possible toxic region of Pm(1–40) has been suggested to be residues 25–35 (Gly_{25}–Ser_{26}–Asn_{27}–Lys_{28}–Gly_{29}–Ala_{30}–Ile_{31}–Ile_{32}–Gly_{33}–Leu_{34}–Met_{35}; Yankner et al., 1990). Within this sequence in C(1–40), four substitutions occur, one nonconservative (Ser_{26}→Pro) and three relatively conservative (Ala_{29}→Val, Ile_{30}→Ala, and Met_{35}–norLeu). Considering that C(1–40) is capable of folding into a β-sheet conformation, it may be that the observed toxicity that is reportedly retained by the peptide (Kowall et al., 1991) is due to structural similarities with Pm(1–40) and that the reduction in neuronal death is due to the multiple changes in the 25–35 region. This is consistent with the report that a full-length β/A4 peptide (residues 1–42) is nontoxic when a soluble monomer but neurotoxic when aggregated (Pike et al., 1991). Perhaps toxicity is due to the conformation assumed by a particular sequence of residues when the polypeptides fold and assemble into cross-β fibrils.

Mutations Affecting Amyloid Formation and Stability. The stability of the β-conformation and the formation and stability of fibrils were greatly enhanced by the single change in sequence of the HCHWA-D peptide (Glu_{22}→Gln). Thus, the β-conformation in Du(1–40) was abundant at pH 10.5 but in the other peptides was either absent [Pm(1–40)] or only marginally present [Ro(1–40)]. Further, Du(1–40) formed numerous fibrils without the need to be stabilized by fixation or by gradual assembly during dialysis, indicating a greater propensity to form a β-sheet. By contrast, Pm(1–40) and Ro(1–40) did not form stable fibrils under aqueous conditions but required pre-fixing similar to that used to stabilize microtubules prior to visualization. Similar instances of increased fibrillogenesis associated with point mutations have been reported, for example, the Leu→Gln mutation of cystatin C (Ghiso et al., 1986) in hereditary cerebral hemorrhage with amyloidosis of the Icelandic type (HCHWA-I) and Asp → Asn of gelsolin peptides in Finnish amyloidosis (Maury & Nurmiaho-Lassila, 1992). It has been previously proposed that the HCHWA-D modification at residue 22 alters the normal cleavage of β/A4 at the neighboring Lys_{16}–Leu_{17} resulting in a redirection of cleavage along an amyloidogenic pathway (Haan et al., 1991). The evidence presented here points to an additional possibility, namely, that the release of an HCHWA-D β/A4 fragment by whatever proteolytic pathway results in a polypeptide species that has a greater tendency to assemble into *stable* amyloid fibrils. This aggregated β-conformation may be necessary for interaction with a receptor, for example, the serpin–enzyme complex (SEC) receptor, which has recently been shown to bind β/A4 fragments (Joslin et al., 1991).

It was recently proposed (Wisniewski et al., 1991) that the HCHWA-D mutation, when present in shorter peptides consisting of residues 1–28 and 21–28, causes an *acceleration* in fibril assembly; however, using electron microscopy and FT-IR, we did not observe any difference in the *rate* of fibril formation between the Dutch variant and the normal human β/A4 analogues. Rather, there was an increase in *stability* of the β-conformation and fibrils of the Dutch variant, and this may be explained by an increased intersheet interaction arising from the Glu_{22}→Gln substitution enhancing the hydrophobicity of the adjacent sequence Leu_{17}–Val_{18}–Phe_{19}–Phe_{20}–Ala_{21}. This region of β/A4 is thought to be an important contributor to amyloid fibril stability (Castaño et al., 1986; Kirschner et al., 1987; Gorevic et al., 1987; Fraser et al., 1991b). In the normal human sequence, the negative charge from Glu_{22} would create electrostatic repulsion between the electron clouds of the Phe_{19}–Phe_{20} aromatic rings in any intersheet packing. It has been shown that Gln or Asn side chains form highly favorable interactions with aromatic side chains (Burley & Petsko, 1986) of Phe or Tyr, which would enhance the intersheet interactions essential for amyloid polymerization. Considering that the carboxyl-terminal, hydrophobic residues of β/A4 may be important in initiating β-sheet formation (Halverson et al., 1990), it is all the more striking that within the extramembranous 28 residues of β/A4, which is thought to direct fibril morphology (Fraser et al., 1991a,b), a single change is sufficient to alter fibril stability.

ACKNOWLEDGMENT

We thank Dr. C. Dahl for peptide synthesis and for designing the C(1–40) peptide and Dr. David Chin for peptide purification.

REFERENCES

Abraham, C. R., Selkoe, D. J., & Potter, H. (1988) *Cell 52*, 487–501.

Abraham, C. R., Shirahama, T., & Potter, H. (1990) *Neurobiol. Aging 11*, 123–129.

Barrow, C. J., & Zagorski, M. G. (1991) *Science 253*, 179–182.

Benowitz, L. I., Rodriguez, W., Paskevich, P., Mufson, E. J., Schenk, D., & Neve, R. L. (1989) *Exp. Neurol. 106*, 237–250.

Burdick, D., Soreghan, B., Kwon, M., Kosmoski, J., Knauer, M., Henschne, A., Yates, J., Cotman, C., & Glabe, C. (1992) *J. Biol. Chem. 267*, 546–554.

Buxbaum, J. D., Gandy, S. E., Ciccetti, P., Ehrilich, M. E., Czernik, A. J., Fracasso, R. P., Ramabhadran, T. V., Unterbeck, A. J., & Greengard, P. (1990) *Proc. Natl. Acad. Sci. U.S.A. 87*, 6003–6006.

Cataldo, A. M., Paskevich, P. A., Kominami, E., & Nixon, R. A. (1991) *Proc. Natl. Acad. Sci. U.S.A. 88*, 10998–11002.

Caputo, C. B., Fraser, P. E., Sobel, I. E., & Kirschner, D. A. (1992) *Arch. Biochem. Biophys. 292*, 199–205.

Castaño, E. M., Ghiso, J., Prelli, F., Gorevic, P. D., Migheli, A., & Frangione, B. (1986) *Biochem. Biophys. Res. Commun. 141*, 782–789.

Dressler, D., Abraham, C. R., Amsterdam, P., & Potter, H. (1989) *Soc. Neurosci. Abstr. 15*, 1041.

Dyrks, T., Weidemann, A., Multhaup, G., Salbaum, J. M., Lemaire, H.-G., Kang, J., Muller-Hill, B., Masters, C. L. & Beyreuther, K. (1988) *EMBO J. 7*, 949–957.

Eanes, E. D., & Glenner, G. G. (1968) *J. Histochem. Cytochem. 16*, 673–677.

Esch, F. S., Keim, P. S., Beattie, E. C., Blacker, R. W., Culwell, A. R., Oltersdorf, T., McClure, D., & Ward, P. J. (1990) *Science 248*, 1122–1124.

Estus, S., Golde, T. E., Kunishita, T., Blades, D., Lowery, D., Eisen, M., Usiak, M., Qu, X., Tabira, T., Greenberg, B. D., & Younkin, S. G. (1992) *Science 255*, 726–728.

Fraser, P. E., Nguyen, J. T., Surewicz, W. K., & Kirschner, D. A. (1991a) *Biophys. J. 60*, 1190–1201.

Fraser, P. E., Duffy, L. K., O'Malley, M. B., Nguyen, J., Inouye, H., & Kirschner, D. A. (1991b) *J. Neurosci. Res. 28*, 474–485.

Ghiso, J., Jensson, O., & Frangione, B. (1986) *Proc. Natl. Acad. Sci. U.S.A. 83*, 2974–2978.

Glenner, G. G., & Wong, C. W. (1984a) *Biochem. Biophys. Res. Commun. 120*, 885–890.

Glenner, G. G., & Wong, C. W. (1984b) *Biochem. Biophys. Res. Commun. 122*, 1131–1135.

Glenner, G. G., Eanes, E. D., Bladen, H. A., Linke, R. P., & Termine, J. D. (1974) *J. Histochem. Cytochem. 22*, 1141–1158.

Goate, A., Chartier-Harlin, M.-C., Mullan, M., Brown, J., Crawford, F., Fidani, L., Giuffra, L., Haynes, A., Irving, N., James, L., Mant, R., Newton, P., Rooke, K., Roques, P., Talbot, C., Pericak-Vance, M., Roses, A., Williamson, R., Rossor, M., Owen, M., & Hardy, J. (1991) *Nature 349*, 704–706.

Golde, T. E., Estus, S., Younkin, L. H., Selkoe, D. J., & Younkin, S. G. (1992) *Science 255*, 728–730.

Gorevic, P. D., Castaño, E. M., Sarma, R., & Frangione, B. (1987) *Biochem. Biophys. Res. Commun. 147*, 854–862.

Haan, J., Hardy, J. A., & Roos, R. A. (1991) *Trends Neurosci. 14*, 231–234.

Halverson, K., Fraser, P. E., Kirschner, D. A., & Lansbury, P. T., Jr. (1990) *Biochemistry 29*, 2639–2644.

Hilbich, C., Kisters-Woike, B., Reed, J., Masters, C. L., & Beyreuther, K. (1991a) *J. Mol. Biol. 218*, 149–163.

Hilbich, C., Kisters-Woike, B., Reed, J., Masters, C. L., & Beyreuther, K. (1991b) *Eur. J. Biochem. 201*, 61–69.

Joachim, C. L., Morris, J. H., & Selkoe, D. J. (1989) *Am. J. Pathol. 135*, 309–319.

Joslin, G., Krause, J. E., Hershey, A. D., Adams, S. P., Fallon, R. J., & Perlmutter, D. H. (1991) *J. Biol. Chem. 266*, 21897–21902.

Kang, J., Lemaire, H.-G., Unterbeck, A., Salbaum, J. M., Masters, C. L., Grzeschik, K.-H., Multhaup, G., Beyreuther, K., & Muller-Hill, B. (1987) *Nature 325*, 733–736.

Kirschner, D. A., Abraham, C. R., & Selkoe, D. J. (1986) *Proc. Natl. Acad. Sci. U.S.A. 83*, 503–507.

Kirschner, D. A., Inouye, H., Duffy, L. K., Sinclair, A., Lind, M., & Selkoe, D. J. (1987) *Proc. Natl. Acad. Sci. U.S.A. 84*, 6953–6957.

Kitaguchi, N., Takahashi, Y., Tokushima, Y., Shiojiri, S., & Ito, H. (1988) *Nature 331*, 530–532.

Koh, J.-Y., Yang, L. L., & Cotman, C. W. (1990) *Brain Res. 533*, 315–320.

Kowall, N. W., Beal, M. F., Busciglio, J., Duffy, L. K., & Yankner, B. A. (1991) *Proc. Natl. Acad. Sci. U.S.A. 88*, 7247–7251.

Levy, E., Carman, M. D., Fernandez-Madrid, I. J., Power, M. D., Leiberburg, I., Van Duinen, S. G., Bots, G. Th. A. M., Luyendijk, W., & Frangione, B. (1990) *Science 248*, 1124–1126.

Mann, D. M. A., & Esiri, M. M. (1989) *J. Neurol. Sci. 89*, 169–179.

Masters, C. L., Multhaup, G., Simms, G., Pottigisser, J., Martins, R. N., & Beyreuther, K. (1985a) *EMBO J. 4*, 2757–2763.

Masters, C. L., Simms, G., Weinman, N. A., Multhaup, G., McDonald, B. L., & Beyreuther, K. (1985b) *Proc. Natl. Acad. Sci. U.S.A. 82*, 4245–4249.

Mattson, M. P., Cheng, B., Davis, D., Bryant, K., Lieberburg, I., Rydel, R. E. (1992) *J. Neurosci. 12*, 376–389.

Maury, C. P. J., & Nurmiaho-Lassila, E.-L. (1992) *Biochem. Biophys. Res. Commun. 183*, 227–231.

McKee, A. C., Kowall, N. W., Beal, M. F., Schumacher, J., & Yankner, B. A. (1991) *Soc. Neurosci. Abstr. 17*, 1294.

Murrell, J., Farlow, M., Ghetti, B., & Benson, M. D. (1991) *Science 254*, 97–99.

Oltersdorf, T., Fritz, L. C., Schenk, D. B., Lieberburg, I., Johnson-Wood, K. L., Beattie, E. C., Ward, P. J., Blacher, R. W., Dovey, H. F., & Sinha, S. (1989) *Nature 341*, 144–147.

Oltersdorf, T., Ward, P. J., Henriksson, T., Beattie, E. C., Neve, R., Lieberburg, I., & Fritz, L. C. (1990) *J. Biol. Chem. 265*, 4492–4497.

Palmert, M. R., Podlisny, M. B., Witker, D. S., Oltersdorf, T., Younkin, L. H., Selkoe, D. J., & Younkin, S. G. (1989) *Proc. Natl. Acad. Sci. U.S.A. 86*, 6338–6342.

Pike, C. J., Walencewicz, A. J., Glabe, C. G., & Cotman, C. W. (1991) *Brain Res. 563*, 311–314.

Podlisny, M. B., Tolan, D., & Selkoe, D. J. (1991) *Am. J. Pathol. 138*, 1423–1435.

Podlisny, M. B., Stephenson, D. T., Frosch, M. P., Tolan, D. R., Lieberburg, I., Clemens, J. A., & Selkoe, D. J. (1992) *Am. J. Pathol.* (in press).

Ponte, P., Gonzalez-DeWhitt, P., Schilling, J., Miller, J., Hsu, D., Greenberg, B., Davis, K., Wallace, W., Lieberburg, I., Fuller, F., & Cordell, B. (1988) *Nature 331*, 525–527.

Quon, D., Wang, Y., Catalano, R., Scardina, J. M., Murakami, K., & Cordell, B. (1991) *Nature 352*, 239–241.

Rozemuller, J. M., Eikelenboom, P., Stam, F. C., Beyreuther, K., & Masters, C. L. (1989) *J. Neuropathol. Exp., Neurol. 48*, 674–691.

Selkoe, D. J. (1991) *Neuron 6*, 487–498.

Selkoe, D. J., Abraham, C. R., Podlisny, M. B., & Duffy, L. K. (1986) *J. Neurochem. 46*, 1820–1834.

Selkoe, D. J., Podlisny, M. B., Joachim, C. L., Vickers, E. A., Lee, G., Fritz, L. C., & Oltersdorf, T. (1988) *Proc. Natl. Acad. Sci. U.S.A. 85*, 7341–7345.

Shivers, B. D., Hilbich, C., Multhaup, G., Salbaum, M., Beyreuther, K., & Seeburg, P. H. (1988) *EMBO J. 7*, 1365–1370.

Sisodia, S. S., Koo, E. H., Beyreuther, K., Unterbeck, A., & Price, D. L. (1990) *Science 248*, 492–495.

Stephenson, D. T., Podlisny, M. B., Games, D., Little, S., Lieberburg, I., Selkoe, D. J., & Clemens, J. A. (1991) *Soc. Neurosci. Abstr. 17*, 1446.

Tanzi, R. E., McClatchey, A. I., Lamperti, E. D., Villa-Komaroff, L., Gusella, J. F., & Neve, R. L. (1988) *Nature 331*, 528–530.

Van Nostrand, W. E., Wagner, S. L., Suzuki, M., Choi, B. H., Farrow, J. S., Cotman, C. W., & Cunningham, D. D. (1989) *Nature 341*, 546–549.

Weidemann, A., Konig, G., Bunke, D., Fischer, P., Salbaum, J. M., Masters, C. L., & Beyreuther, K. (1989) *Cell 57*, 115–126.

Whitson, J. S., Selkoe, D. J., & Cotman, C. W. (1989) *Science 243*, 1488–1490.

Wisniewski, T., Ghiso, J., & Frangione, B. (1991) *Biochem. Biophys. Res. Commun. 179*, 1247–1254; *180*, 1528 (a corrigendum).

Yamada, T., Sasaki, H., Furuya, H., Miyata, T., Goto, I., & Sakaki, Y. (1987) *Biochem. Biophys. Res. Commun. 149*, 665–671.

Yamada, T., Sasaki, H., Dohura, K., Goto, I., & Sakaki, Y. (1989) *Biophys. Biochem. Res. Commun. 158*, 906–912.

Yamaguchi, H., Hirai, S., Morimatsu, M., Shoji, M., & Nadazato, Y. (1989a) *Acta Neuropathol. 77*, 314–319.

Yamaguchi, H., Nakazato, Y., Hirai, S., Shoji, M., & Harigaya, Y. (1989b) *Am. J. Pathol. 135*, 593–597.

Yankner, B. A., Dawes, L. R., Fisher, S., Villa-Komaroff, L., Oster-Granite, M. L., & Neve, R. L. (1989) *Science 245*, 417–420.

Yankner, B. A., Duffy, L. K., & Kirschner, D. A. (1990) *Science 250*, 279–282.